Please cite this article in press as:
Ye, H. and Liu, R. (2016) A multiphase optimal control method for multi-train control and scheduling on railway lines. **Transportation Research Part B**. In press.

A multiphase optimal control method for multi-train control and scheduling on railway lines

Hongbo Ye and Ronghui Liu[1]
Institute for Transport Studies, University of Leeds, United Kingdom

Abstract

We consider a combined train control and scheduling problem involving multiple trains in a railway line with a predetermined departure/arrival sequence of the trains at stations and meeting points along the line. The problem is formulated as a multiphase optimal control problem while incorporating complex train running conditions (including undulating track, variable speed restrictions, running resistances, speed-dependent maximum tractive/braking forces) and practical train operation constraints on departure/arrival/running/dwell times. Two case studies are conducted. The first case illustrates the control and scheduling problem of two trains in a small artificial network with three nodes, where one train follows and overtakes the other. The second case optimizes the control and timetable of a single train in a subway line. The case studies demonstrate that the proposed framework can provide an effective approach in solving the combined train scheduling and control problem for reducing energy consumption in railway operations.

Keywords: Optimal control; Energy; Railway; Moving block; Train trajectory; Timetable rescheduling.

1. Introduction

Energy consumption in the railway industry is not only a concern for railway operators, but also attracts attentions from the academia. It is a consensus that a well-designed train control strategy could significantly reduce the energy consumption during the train run.

[1] Corresponding author. Email: R.Liu@its.leeds.ac.uk; Tel: +44 113 343 5338.

The train control problem is usually described as minimising the energy consumption of a train travelling from one station to the next within a given time period. The optimal control theory is a powerful tool for analysing such problem. In the pioneer work of Ichikawa (1968), the continuous train control problem under speed restriction was analysed as an optimal control problem with bounded state variables. Milroy (1980) suggested that, for short journeys, the optimal train control strategy consists of three control stages: maximum acceleration, coasting, and maximum braking. Asnis et al. (1985) and Howlett (1990) found that, for long journeys, an additional speedholding stage should be included, leading to an optimal sequence of acceleration, speedholding, coasting, and deceleration. Later research showed that these four distinct modes can be used to create optimal control strategies for very complex train operation problems involving variable track gradient (including steep climbs and steep descents), variable speed limit, complex train characteristics, and power regeneration (Albrecht et al., 2015b, 2015c; Howlett, 2000; Khmelnitsky, 2000; Liu and Golovitcher, 2003).

Different to the above-mentioned continuous train control problems, for some diesel locomotives, only discrete throttle settings are available. There, the speed may not be perfectly held for the speedholding operation. Under the discrete settings, Cheng and Howlett (1992, 1993) optimised the switching points of a prescribed number of control phases and showed that, in the simplest case of level track without speed limit, the speedholding can be approximated to any desired accuracy by a sequence of coast-power pairs. The discussion was further extended to the case of undulating tracks (Howlett, 1996; Howlett and Cheng, 1997), variable speed limits (Pudney and Howlett, 1994) and a combination of both (Cheng et al., 1999). The state-of-the-art review on both continuous and discrete train control problems can be found in Howlett et al. (2009) and Albrecht et al. (2015b, 2015c).

Efficient algorithms are essential for implementing optimal train control in real-life train operations. Numerical methods based on the Pontryagin's maximum principle has been well developed by Albrecht et al. (2015b, 2015c), Howlett et al. (2009), Khmelnitsky (2000) and Liu and Golovitcher (2003), and some of them have been implemented in the practical real-time driver advisory systems such as the Energymiser[2]. Genetic algorithms have been used to determine the optimal starting points and the lengths of coasting phases (Chang and Sim, 1997; Wong and Ho, 2004). Discretisation and approximation are often used to convert the original optimal train control formulation to the mathematical programming problems,

[2] http://www.ttgtransportationtechnology.com/energymiser/

such as dynamic programming method (Effati and Roohparvar, 2006; Franke et al., 2000; Ko et al., 2004; Vasak et al., 2009), linear programming method (Effati and Roohparvar, 2006; Wang et al., 2013, 2014) and pseudospectral method (Wang and Goverde, 2016; Wang et al., 2013, 2014). There are also numerical methods that don't belong to the above-mentioned types. For example, in Gu et al. (2014), the whole section between two stations is first divided into several subsections according to gradients and speed limits. The optimal control scheme on each of these subsections is derived and then used to obtain the control strategy for the complete journey through nonlinear programming. For the classical train control problems, the numerical methods based on the Pontryagin's maximum principle might be generally superior to other numerical methods mentioned above; however, for optimal train control in a general network, which is our focus in this paper, there is so far no efficient algorithms based on the Pontryagin's maximum principle, and in this case other numerical methods may be able to provide satisfying solutions.

In the classical train control problem, a single train is considered to run freely between two stations with prescribed journey times. However, this framework can face challenges in a complex and busy railway network. As it was argued by Albrecht et al. (2015b),

> *"… the most pressing research challenges for the future in this area are to develop* optimal control policies for trains travelling in the same direction on the same line in such a way that safe separation is maintained between trains. On busy rail networks, solution of the train separation problem relates to and depends on integrated scheduling and control policies to ensure that train movements are both energy-efficient and effectively *coordinated."*

The quote above raises two research gaps: the control of multiple trains running simultaneous on the same track, and the integration of train scheduling with optimal train control.

It happens in both fixed-block and moving-block systems that two or more trains can run sufficiently close to each other on the same track, and thus affect each other's operation. For example, when a train is expected to arrive at its frontal station ahead of schedule at full speed, it can slow down to save energy; however, the decision to slow down may affect the operation and thus the energy consumption of the train following it. In this case, the trajectories of both trains would be better optimised simultaneously. Research on this issue is still limited so far, as noted in Açıkbaş and Söylemez (2008), Albrecht et al. (2015a), Lu and Feng (2011), Miyatake and Ko (2010), Wang et al. (2014), Yan et al. (2016) and Zhao et al. (2015). Specifically, Lu and Feng (2011) used genetic algorithm to optimise the control strategies of leading and following trains in a four-aspect fixed-block signalling system. Wang et al. (2014) considered two trains traversing a single track following each other, under both fixed and moving block systems. They used the mixed integer linear programming approach to formulate the problems, and then solved the control strategies sequentially (the control of the leading train is solved first and then fixed when solving the control of the following train) or simultaneously. Albrecht et al. (2015a) provided theoretical analysis and solution algorithm for the train separation problem based on the optimal control theory, in which two trains were operated under the fixed-block system with specified starting and finishing times on level tracks without speed limit. Yan et al. (2016) developed an online distributed cooperative approach for optimising the control of multiple trains based on model predictive control and ant colony optimisation, where the trains are assumed to share their states and decisions with each other through radio.

Energy consumption is a big concern for the train operators as it directly affects the operators' profit margin. However, when it comes to train scheduling (over a large railway network), time efficiency is usually the first priority (Cacchiani and Toth, 2012; Cacchiani et al., 2014; Guo et al., 2016). There have been studies where energy consumption is incorporated in the scheduling process at an aggregated level. For example, in Medanic and Dorfman (2002) and Ghoseiri et al. (2004), the energy cost of a train running on a railway section is assumed to be a convex function of the average velocity of that train on that section[3]. If a more precise estimation on the energy consumption is expected, knowing the average speed is not enough. Instead, the detailed train running information at each time and location of the journey, including traction and braking forces, speed, and resistance, are required. However, these details are difficult to incorporate in the currently widely-used scheduling methods such as mathematical programming (Carey, 1994; Higgins et al., 1996) and discrete event simulation (Dorfman and Medanic, 2004; Li et al., 2008). Regarding this issue, attempts have been made in Yang et al. (2012) and Goodwin et al. (2016), where the railway is operated under the fixed-block systems, and the solution is obtained by the genetic algorithm. Wang and Goverde (2016) considered the control of an individual train to minimise energy consumption and delay, while the train trajectory is restricted by the time/speed windows at specific locations of the track. A special case of this combined scheduling and control problem is to design the energy-efficient timetable in a metro line, as in Gupta et al. (2016), Li and Lo (2014a, 2014b), Su et al. (2013), Xu et al. (2016), Yang et al.

[3] It was confirmed in Albrecht et al. (2016) that the energy consumption on level track is a strictly decreasing and strictly convex function of journey time. A new explicit formula was also provided in their paper for the rate of change of energy consumption with respect to journey time.

(2015, 2016) and Yin et al. (2016), just to name a few.

In this paper, we intend to optimise the control strategies of multiple trains in a moving-block railway line to achieve the minimum energy consumption. A multiphase optimal control problem (MOCP) is established to solve the problem. The MOCP doesn't necessitate a fixed train schedule; instead, it requires only a predetermined time order of all trains arriving and leaving all stations and meeting points. As a result, we could obtain not only optimal train control strategies but also an optimal train schedule satisfying this given sequence of arrivals and departures. The proposed MOCP framework is flexible, in that it allows the track gradients and speed limits to change with location, and the running resistances and maximum tractive/braking forces to change with speed. Besides, it can incorporate the train operation constraints with respect to, for example, the safe train separation, the arrival/departure/dwelling times at stations, and the inter-station running times. An additional notable feature of the proposed method is that, to formulate and solve the MOCP, no prior information is required on the structure of the optimal control strategy. The proposed methodology will be demonstrated by two case studies. The first example considers a scenario where a fast train follows and overtakes a slow train in the moving block system. The second example considers the integrated design of schedule and control for a single train across multiple stations.

The rest of this paper is organised as follows. Section 2 introduces the traditional single-train control problem, based on which the MOCP for multi-train scheduling and control are established in Section 3. Two cases are studied in Section 4, and conclusions are drawn in Section 5. For reference, Appendix A and Appendix B respectively provide the solution algorithm and parameter settings of the software package used in the case studies.

2. Optimal control of a single train

In this section, we introduce the traditional single-train control problem. The train is treated as a point of mass M [4]. We choose time t as the independent variable, and the train's location and speed as dependent variables, denoted $x(t)$ and $v(t)$ respectively. For

[4] Howlett and Pudney (1995) have pointed out that the formulation for point-mass train is also applicable for the distributed-mass train by replacing the original gradient profile with a density-weighted one.

simplicity, we omit t and write $x = x(t)$ and $v = v(t)$ hereafter. The train movement is modelled as follows (Jaekel and Albrecht, 2014; Rochard and Schmid, 2000):

$$\dot{x} = v \tag{1}$$

$$\dot{v} = \frac{1}{M}\left(F - B - R(v) - G(x)\right) \tag{2}$$

where $\dot{x} = dx/dt$ and $\dot{v} = dv/dt$ are the respective time derivatives; $F = F(t)$ and $B = B(t)$ are respectively the instantaneous tractive and braking forces applied to the train; $R(v)$ is the sum of mechanical and aerodynamic resistances at speed v; and $G(x)$ is the force caused by the track gradient at location x (positive for upgrade and negative for downgrade).

The maximum speed that a train can achieve at any specific location x is restricted by the local speed restriction on the track, denoted by $\bar{v}(x)$, i.e.,

$$0 \le v \le \bar{v}(x) \tag{3}$$

The maximum tractive force and maximum braking force that a train can apply are not necessarily constants, but decreasing functions of the train's instantaneous speed v, written as $\bar{F}(v)$ and $\bar{B}(v)$, respectively. So the tractive and breaking forces should satisfy

$$0 \le F \le \bar{F}(v) \tag{4}$$

and

$$0 \le B \le \bar{B}(v) \tag{5}$$

The resistive force is usually formulated as a quadratic function of speed, known as the Davis formula (Jaekel and Albrecht, 2014; Rochard and Schmid, 2000):

$$R(v) = av^2 + bv + c \tag{6}$$

where a, b and c are train-specific constants. The track gradient $\theta(x)$ is defined as the ratio of the vertical rise to the horizontal distance traversed. When $\theta(x)$ is small, the force caused by $\theta(x)$ at location x is given by

$$G(x) = Mg\sin(\arctan\theta(x)) \approx Mg\sin\theta(x)\,^{5} \tag{7}$$

where g is the gravitational constant.

The single train control problem is then described as minimising its energy consumption when traversing a predetermined distance from x_0 to x_f within a predetermined time interval from t_0 to t_f, i.e.,

$$\min_{F(t),B(t)} \int_{t_0}^{t_f} F(t)v(t)dt$$

s.t. $x(t_0) = x_0$, $x(t_f) = x_f$, $v(t_0) = v(t_f) = 0$, and Eqs. (1) - (7)

3. Multiphase optimal control framework for multi-train control and scheduling in moving block systems

In this section, we will provide the formulation for the multi-train control and scheduling problem. Specifically, Section 3.1 will introduce basic settings of the system as well as basic definitions, based on which Section 3.2 will discuss the process of formulating the MOCP in detail.

3.1. Preliminaries

Consider a unidirectional railway line[6] (Figure 1) which consists of a set $\mathbb{S}$ of nodes, $\mathbb{S} = \{1,2,\cdots,S\}$, where each node represents either a meeting point or a station. Denote by X_s the location of node s, and naturally we assume that $X_1 < X_2 < \cdots < X_S$. N trains, numbered from 1 to N, traverse the line from node 1 to node S. Suppose that the capacities of nodes 1 and S are at least N, but could be smaller for the intermediate nodes 2 to $S-1$. The railway line is operated under the moving block signalling system[7], and overtaking is allowed at the intermediate nodes.

---

[5] If $\theta(x)$ is defined by the angle, then one will naturally have $G(x) = Mg\sin\theta(x)$.

[6] Extension from the one-way line to the general train networks with bi-directional traffic would be straightforward.

[7] Theoretically speaking, the modelling technique proposed subsequently can also be adapted to model fixed-block systems, which will require additional specifications on the time sequence of trains entering and leaving all blocks.

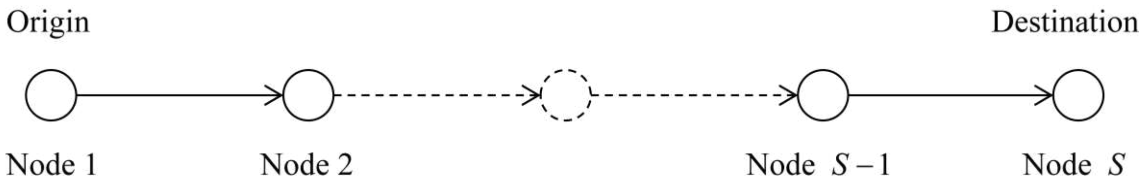

Figure 1. Illustration of the unidirectional single-line railway

Our main goal is to optimise the control strategies of the N trains. Since the intermediate nodes are involved in the train journey, scheduling at these intermediate nodes will be considered as well. As a result, we will have a combined train control and scheduling problem which involves multiple trains and multiple nodes.

To formulate the problem, we divide the whole time horizon, from the departure of the first train from node 1, to the arrival of the last train at node S, into a finite number of time intervals by some criteria, and each of these time intervals is called a "phase". In each phase, the train movement can be described according to Section 2, with specific boundary constraints and extra train separation constraints. Extra linkage constraints are then used to connect the phases and form a multiphase optimal control problem (MOCP).

We define each departure (D) or arrival (A) of each train at each node as an "event". Specially, a train passing a node without stop would be treated as an arrival event followed immediately by a departure event. Therefore the total number of events is $2N(S-1)$. By placing all the events in a time-ascending order, we call the resultant sequence a "D/A-sequence". Notably, the overtaking plans are specified by the D/A-sequence. To fit our problem into a standard MOCP, we assume that the D/A-sequence is predetermined, fixed, and conflict-free; however, the exact timings of the events are undetermined and thus will be the decision variables. It is worth mentioning that, knowing the D/A-sequence is less restrictive than knowing the exact timings of the events, so the latter is a special case of the former, and the former is obviously more difficult to solve than the latter.

Define phase p as the time interval between the p-th and (p+1)-th events[8], and thus the total number of phases is $P = 2N(S-1)-1$. In addition, we assume that all the trains have to

[8] Under certain circumstances, some adjacent phases can be combined to reduce the number of phases and thus reduce the complexity of the problem. See Section 4.1 for an example.

reach zero speed[9] (but not necessarily dwell) at each node. Then the status of each train in phase p is categorised in Table 1, based on its locations at the initial time $t_0^{(p)}$ and terminal time $t_f^{(p)}$ of this phase. Such categorisation is for the convenience of specifying boundary constraints w.r.t. each individual train in each phase, which will be given in Table 3 later. Notably, such categorisation is unrelated to node index s since the latter would not affect the form of the boundary constraints.

Table 1. Categorisation of train status for a typical individual train in phase p

Category	Train status at $t_0^{(p)}$	Train status at $t_f^{(p)}$
1	Departing from node s	Arriving at node $s+1$
2	Departing from node s	Not yet arrived at node $s+1$
3	Already departed from node s	Arriving at node $s+1$
4	Already departed from node s	Not yet arrived at node $s+1$
5	Waiting for departure at the origin (node 1)	
6	Stopping at the intermediate nodes 2 to $S-1$	
7	Stopping at the destination (node S)	

We now use the following example to illustrate the concepts established in this subsection.

Example 1. Consider two trains travelling from node 1 to node 3 through node 2. Their trajectories and arrival/departure at each node are illustrated in

Figure **2**. Each train corresponds to four events, which are: departure from node 1, arrival at node 2, departure from node 2, and arrival at node 3. As a result, the whole time horizon is divided into 7 phases. The category that each train belongs to in each phase is summarised in Table 2. □

[9] In Scenario 2 of Section 4.1, the zero-speed assumption will be relaxed, and the boundary constraints will be modified accordingly.

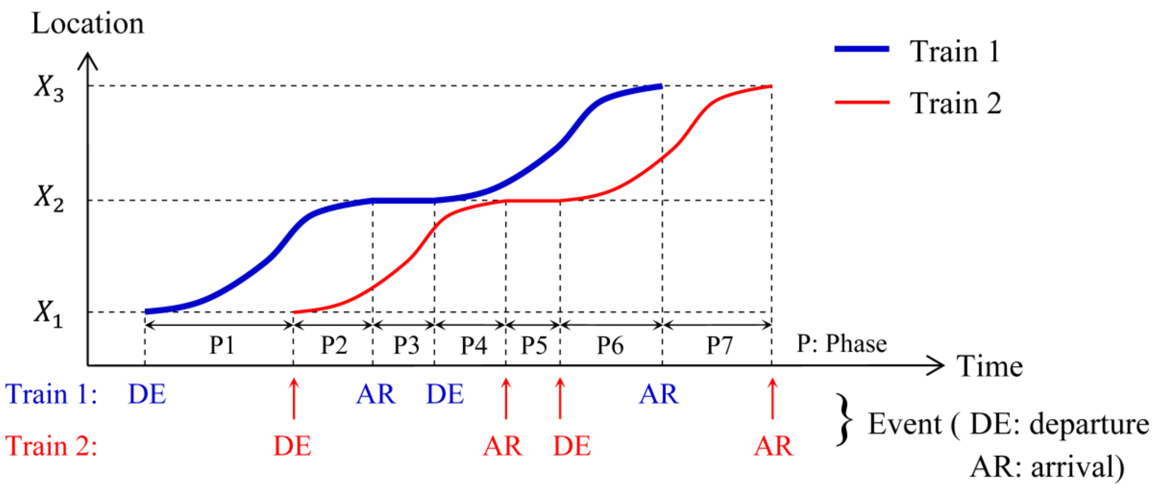

Figure 2. A two-train three-node example: events, D/A-sequence and phases.

Table 2. Categorisation of train status in each phase in Example 1

Phase	P1	P2	P3	P4	P5	P6	P7
Train 1	2	3	6	2	4	3	7
Train 2	5	2	4	3	6	2	3

3.2. Formulating the MOCP for multi-train control and scheduling

With the description in Section 3.1, we are now ready to formulate the MOCP for the general train control and scheduling problem. Let $x_n^{(p)} = x_n^{(p)}(t)$, $v_n^{(p)} = v_n^{(p)}(t)$, $F_n^{(p)} = F_n^{(p)}(t)$ and $B_n^{(p)} = B_n^{(p)}(t)$ denote, respectively, the location, speed, tractive force and braking force of train n at time t within phase p. The objective is to minimise the total energy consumption, which is formulated as follows:

$$\min \sum_{n\in\mathbb{N}} \sum_{p\in\mathbb{P}} \int_{t_0^{(p)}}^{t_f^{(p)}} F_n^{(p)}(t) v_n^{(p)}(t)\, dt, \quad \mathbb{N} = \{1, 2, \cdots, N\}, \quad \mathbb{P} = \{1, 2, \cdots, P\} \tag{8}$$

We assume that the train would not apply traction and thus not consume energy when it stops at a node (i.e. categories 5-7). Furthermore, we allow the train mass to change when and only when it stops at the train stations (due to boarding and alighting of passengers). Then during phase p, for a train n belonging to categories 5-7, its movement equations are given as follows:

$$\dot{x}_n^{(p)} = 0 \tag{9}$$

$$\dot{v}_n^{(p)} = 0 \tag{10}$$

with

$$v_n^{(p)} = 0, \quad F_n^{(p)} = 0, \quad B_n^{(p)} = 0 \tag{11}$$

For a train n belonging to categories 1-4, its movement equations are given as follows:

$$\dot{x}_n^{(p)} = v_n^{(p)} \tag{12}$$

$$\dot{v}_n^{(p)} = \frac{1}{M_n^{(p)}}\left(F_n^{(p)} - B_n^{(p)} - R_n\left(v_n^{(p)}\right) - G\left(x_n^{(p)}\right)\right) \tag{13}$$

subject to constraints (14)-(16):

$$0 \le F_n^{(p)} \le \bar{F}_n\left(v_n^{(p)}\right) \tag{14}$$

$$0 \le B_n^{(p)} \le \bar{B}_n\left(v_n^{(p)}\right) \tag{15}$$

$$0 \le v_n^{(p)} \le \bar{v}\left(x_n^{(p)}\right) \tag{16}$$

where $M_n^{(p)}$ is the constant train mass during phase p; $R_n(v)$, $\bar{F}_n(v)$ and $\bar{B}_n(v)$ are respectively the running resistance, maximum tractive force and maximum braking force of train n at speed v.

Remark. For the specific software package we use in the case studies for solving the proposed models, if the upper bounds in Eqs. (14)-(16) are not constant, then these constraints should be expressed as the combination of the following path constraints

$$F_n^{(p)} - \bar{F}_n\left(v_n^{(p)}\right) \le 0, \quad B_n^{(p)} - \bar{B}_n\left(v_n^{(p)}\right) \le 0, \quad v_n^{(p)} - \bar{v}\left(x_n^{(p)}\right) \le 0$$

and the following boundary constraints

$$F_n^{(p)} \ge 0, \quad B_n^{(p)} \ge 0, \quad v_n^{(p)} \ge 0$$

For safety reasons, a distance above the safety margin should be maintained between two consecutive trains running on the same railway section, where the railway section is defined as the railway track between two adjacent nodes. To meet this requirement, for each train pair (i, j) in phase p, where train j is the immediate follower of train i, we add a path constraint as follows:

$$x_i^{(p)} - x_j^{(p)} \geq d_j \text{, if train } j \text{ follows train } i \text{ on the same section during phase } p \quad (17)$$

where d_j is the minimum braking distance of train j. This minimum distance is not necessarily constant; it could be a function of the states of both trains (Chen et al., 2016; Wang et al., 2014).

Let $s_n^{(p)}$ be the node where train n departs from (categories 1-4) or dwells at (categories 5-7) in phase p, i.e. $s_n^{(p)} = \max\left\{s \in \mathbb{S} : X_s \leq x_n^{(p)}\left(t_0^{(p)}\right)\right\}$. According to the categorisation in Table 1, the boundary constraints on each train's initial and terminal states in each phase, are specified and summarised in Table 3. Notably, for a train belonging to categories 2 and 4, when the node that it is heading to is fully occupied, the safety margin should be considered. Then the boundary constraint on the terminal location of a train in categories 2 and 4 is formulated as follows:

$$x_n^{(p)}\left(t_f^{(p)}\right) \in \begin{cases} \left[X_{s_n^{(p)}}, X_{s_n^{(p)}+1} - d_n\right], & \text{if node } s_n^{(p)}+1 \text{ is fully occupied} \\ \left[X_{s_n^{(p)}}, X_{s_n^{(p)}+1}\right], & \text{otherwise} \end{cases} \quad (18)$$

Table 3. Boundary constraints of train n in phase p

Category	Initial location $x_n^{(p)}\left(t_0^{(p)}\right)$	Initial speed $v_n^{(p)}\left(t_0^{(p)}\right)$	Terminal location $x_n^{(p)}\left(t_f^{(p)}\right)$	Terminal speed $v_n^{(p)}\left(t_f^{(p)}\right)$
1	$= X_{s_n^{(p)}}$	$= 0$	$= X_{s_n^{(p)}+1}$	$= 0$
2	$= X_{s_n^{(p)}}$	$= 0$	Eq. (18)	free
3	$\in \left[X_{s_n^{(p)}}, X_{s_n^{(p)}+1}\right]$	free	$= X_{s_n^{(p)}+1}$	$= 0$
4	$\in \left[X_{s_n^{(p)}}, X_{s_n^{(p)}+1}\right]$	free	Eq. (18)	free
5-7	$= X_{s_n^{(p)}}$	$= 0$	$= X_{s_n^{(p)}}$	$= 0$

Finally, to connect two consecutive phases p and $p+1$, we define the linkage constraints as follows:

$$\begin{cases} t_f^{(p)} = t_0^{(p+1)} \\ x_n^{(p)}\left(t_f^{(p)}\right) = x_n^{(p+1)}\left(t_0^{(p+1)}\right), \quad n \in \mathbb{N}, \quad p \in \{1, \cdots, P-1\} \\ v_n^{(p)}\left(t_f^{(p)}\right) = v_n^{(p+1)}\left(t_0^{(p+1)}\right) \end{cases} \tag{19}$$

Eqs. (8)-(19) together with Table 1 and Table 3 provide the basic multiphase optimal control framework for optimising the train control and schedule and achieving minimum energy consumption of the multi-train system. In practical train operations, additional constraints may be applied, e.g., the departure/arrival time window at a station, the minimum/maximum dwell time at a station, and the maximum running time between any two stations. For simplicity, the explicit multiphase optimal control formulations regarding these additional constraints are not provided in this section; instead, some of them will be considered and formulated in the case studies in Section 4.

To end this subsection, we summarise the procedure of formulating a multi-train multi-node control and schedule optimisation problem into a MOCP as follows:

Step 1: given the D/A-sequence, categorising the status of each train in each phase according to Table 1;

Step 2: based on the train status, formulating the objective function (8) and constraints (9)-(16), (19);

Step 3: referring to the D/A-sequence, listing the leading-following relationship on each railway section in each phase;

Step 4: based on the train status and leading-following relationship, formulating the constraints in (17), and the boundary conditions based on Table 3;

Step 5: if any, formulating the additional constraints with respect to departure time, dwell time, running time, etc.

The MOCP can then be solved by the general-purpose optimal control software packages, such as GPOPS (Benson et al., 2006; Garg et al., 2010, 2011a, 2011b; Rao et al., 2010) and PSOPT (Becerra, 2010).

4. Case studies

In this section, we demonstrate the potential of the proposed framework in solving two practical problems combining train control and scheduling. The Matlab software package

GPOPS Version 5.1, which is based on the Radau pseudospectral method (RPM), is used to obtain the solutions. A brief introduction to RPM is presented in Appendix A. The key parameters used in GPOPS are explained in Appendix B, and their values chosen in the case studies are provided in Table B.1. The programs run on Matlab R2015a on a desktop PC with 8G RAM and a 3.2GHz CPU.

4.1. Case study 1: multi-train multi-node control optimisation in a moving block railway system

Consider the railway line in Figure 1 with three nodes, where nodes 1 and 3 are stations and node 2 is a meeting point. The capacity of each node is two. The locations of nodes 1, 2 and 3 are 0km, 40km and 80km, respectively. The speed limit on the track is uniform at $\bar{v} = 180$km/h, and the track gradients are given in Table 4. Two trains are scheduled to travel from node 1 to node 3. The two trains are identical in characteristics such as mass ($M = 6\times10^5$kg), resistance, maximum tractive force and maximum braking force, shown as follows, where v is in km/h, and $\bar{F}(v)$, $\bar{B}(v)$ and $R(v)$ are in kN. The safety distance is set at $d = 2$km for both trains.

$$\bar{F}(v) = \begin{cases} 140, & 0 \le v \le 90 \\ 140 - 0.9(v-90), & 90 < v \le 180 \end{cases}$$

$$\bar{B}(v) = \begin{cases} 200, & 0 \le v \le 60 \\ 200 - 0.8(v-60), & 60 < v \le 180 \end{cases}$$

$$R(v) = 1.269\times10^{-3}v^2 + 0.101v + 11.4$$

Table 4. Track gradient in the form: gradient (‰)/subsection start – end location (m)

0/0-2284	-4.2/2284-3871	2/3871-6094	16.7/6094-8181	0/8181-10323	1.7/10323-13750
0/13750-15711	13.3/15711-19314	0/19314-21222	-5.6/21222-23609	-8.3/23609-27504	-3.3/27504-30127
-8.3/30127-32778	-2.5/32778-36003	0/36003-38091	0.5/38091-40000	0/40000-42284	-4.2/42284-43871
2/43871-46094	16.7/46094-48181	0/48181-50323	1.7/50323-53750	0/53750-55711	13.3/55711-59314
0/59314-61222	-5.6/61222-63609	-8.3/63609-67504	-3.3/67504-70127	-8.3/70127-72778	-2.5/72778-76003
0/76003-78091	0.5/78091-80000				

We consider two scenarios, named Scenario 1 and Scenario 2, in this case study. In Scenario 1, the two trains run according to a planned timetable. Later in Scenario 2, the timetable is modified in response to an incident which occurred during the train run, in which the controls of both trains are recalculated, resulting in rescheduling at the intermediate node 2.

For Scenario 1, the planned ("original") timetable is given in Table 5. Since the journey time and train characteristics are identical for both trains, and their departure times are far apart, we can expect that the train separation constraint is redundant[10] and the two trains' optimal control strategies are identical. Thus the problem is simply solved as a single-phase optimal control problem according to Section 2. The parameter settings for GPOPS are given in Table B.1 (column I). The computation time is 115 seconds.

Table 5. Original timetable

Train	Departure time at node 1	Arrival time at node 3
1	08:00	08:35
2	08:05	08:40

The optimal speed profile and control strategy of each train under the original timetable is illustrated in Figure 3. The optimal control profile (positive for traction and negative for braking) starts with maximum traction, and ends with coasting followed by maximum braking. The expected speedholding operation is not perfectly realized; instead, it is approximated by a mixture of coast-power pairs and speedholding. It might be because that the speedholding corresponds to the singular arc of the train control problem given in Section 2 (Albrecht et al., 2015b; Howlett, 2000; Khmelnitsky, 2000; Liu and Golovitcher, 2003), and it has been known that the singular arc may not be perfectly estimated by the so-called direct method including RPM for solving the optimal control problems (Betts, 2010; Garg, 2011; Patterson and Rao, 2014; Rao et al., 2010). To obtain a high-accuracy speedholding operation by RPM, one may explicitly provide the singular arc conditions as path constraints (Betts, 2010; Patterson and Rao, 2014) in the original optimal control formulation. Regarding this, Howlett et al. (2009) and Albrecht et al. (2015b, 2015c) have proposed explicit numerical methods that can be used to find the initial and final points of a singular speedholding phase; however, it requires and is worth further investigation in the future whether their method can be combined with RPM and help identify the speedholding phases under the complex settings in this paper with multiple trains and/or multiple nodes.

[10] It can be easily verified by checking the optimised trajectories of the two trains in Figure 3.

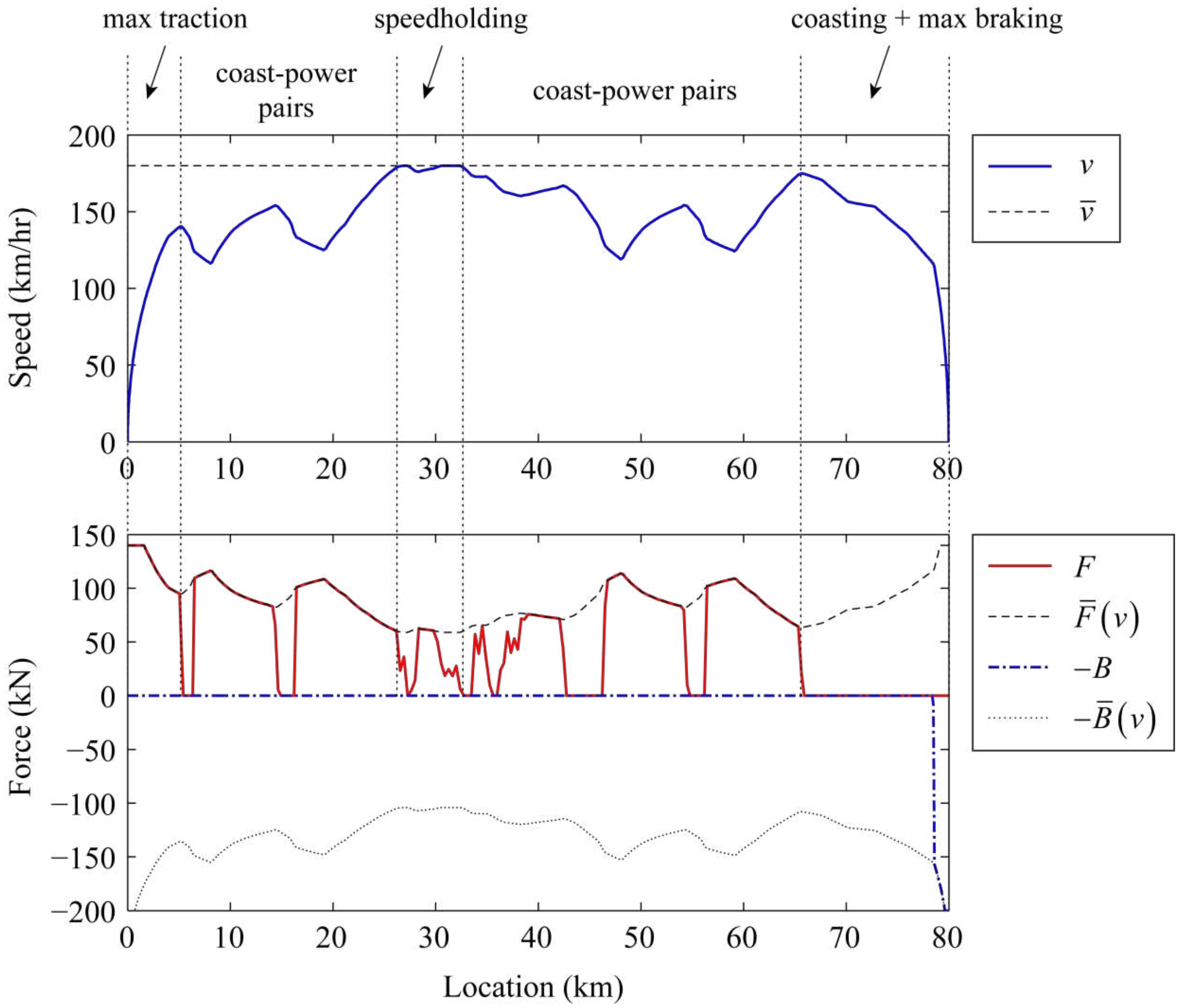

Figure 3. Optimal train speed profile and control strategy under the original schedule

For Scenario 2, we suppose that, when both trains are running as planned, a malfunction happens on train 1 at time $T_0' = 08{:}10$, when the location and speed of train 1 are $X_{10}' = 19144\text{m}$ and $V_{10}' = 35.4\text{m/s}$, and that of train 2 are $X_{20}' = 7611\text{m}$ and $V_{20}' = 33.1\text{m/s}$. Due to this malfunction, the maximum tractive force of train 1 is altered to be

$$\hat{F}(v) = \begin{cases} 70, & 0 \le v \le 90 \\ 70 - 0.9(v - 90), & 90 < v \le 180 \end{cases}$$

where v is in km/hr and $\hat{F}(v)$ in kN. As a result, train 1 is not able to reach node 3 as scheduled. To reduce the delay on train 2, train 1 is asked to stop at node 2 to let train 2 overtake, and the arrival times of both trains at node 3 are adjusted to be $T_{1f}' = 08{:}50$ and $T_{2f}' = 08{:}45$, respectively.

To optimise the control of both trains under this incident, as illustrated in Figure 4, we define five events, which are (i) the occurrence of malfunction at time T_0', (ii) the arrival of train 1 at node 2, (iii) the departure of train 1 from node 2, (iv) the arrival of train 2 at node 3 at time T_{2f}', and (v) the arrival of train 1 at node 3 at time T_{1f}'. Then the whole time horizon $\left[T_0', T_{1f}'\right]$ is divided into four phases, and the MOCP is formulated as follows.

$$\min \sum_{p=1}^{4} \sum_{n=1}^{2} \int_{t_0^{(p)}}^{t_f^{(p)}} F_n^{(p)}(t) v_n^{(p)}(t) dt$$

subject to the following sets of constraints:

(a) the train movement dynamic constraints:

$$\dot{x}_n^{(p)} = \begin{cases} 0 & \text{if } (n=1, p=2) \text{ or } (n=2, p=4) \\ v_n^{(p)} & \text{otherwise} \end{cases}, \quad n=1,2, \quad p=1,2,3,4$$

$$\dot{v}_n^{(p)} = \begin{cases} 0 & \text{if } (n=1, p=2) \text{ or } (n=2, p=4) \\ \dfrac{1}{M}\left[F_n^{(p)} - B_n^{(p)} - R\left(v_n^{(p)}\right) - G\left(x_n^{(p)}\right)\right] & \text{otherwise} \end{cases}, \quad n=1,2, \quad p=1,2,3,4$$

(b) the boundary constraints:

Phase 1: $t_0^{(1)} = T_0'$

$$x_1\left(t_0^{(1)}\right) = X_{10}', \quad x_1\left(t_f^{(1)}\right) = X_2, \quad v_1\left(t_0^{(1)}\right) = V_{10}', \quad v_1\left(t_f^{(1)}\right) = 0$$

$$x_2\left(t_0^{(1)}\right) = X_{20}', \quad x_2\left(t_f^{(1)}\right) \in \left[X_{20}', X_2 - d\right], \quad v_2\left(t_0^{(1)}\right) = V_{20}', \quad v_2\left(t_f^{(1)}\right) \geq 0$$

Phase 2: $x_1\left(t_0^{(2)}\right) = X_2, \quad x_1\left(t_f^{(2)}\right) = X_2, \quad v_1\left(t_0^{(2)}\right) = 0, \quad v_1\left(t_f^{(2)}\right) = 0$

$$x_2\left(t_0^{(2)}\right) \in \left[X_{20}', X_2 - d\right], \quad x_2\left(t_f^{(2)}\right) \in \left[X_2 + d, X_3\right], \quad v_2\left(t_0^{(2)}\right) \geq 0, \quad v_2\left(t_f^{(2)}\right) \geq 0$$

Phase 3: $t_f^{(3)} = T_{2f}'$

$$x_1\left(t_0^{(3)}\right) = X_2, \quad x_1\left(t_f^{(3)}\right) \in \left[X_2, X_3 - d\right], \quad v_1\left(t_0^{(3)}\right) = 0, \quad v_1\left(t_f^{(3)}\right) \geq 0$$

$$x_2\left(t_0^{(3)}\right) \in \left[X_2 + d, X_3\right], \quad x_2\left(t_f^{(3)}\right) = X_3, \quad v_2\left(t_0^{(3)}\right) \geq 0, \quad v_2\left(t_f^{(3)}\right) = 0$$

Phase 4: $t_0^{(4)} = T_{2f}', \quad t_f^{(4)} = T_{1f}'$

$$x_1\left(t_0^{(4)}\right) \in \left[X_2, X_3 - d\right], \quad x_1\left(t_f^{(4)}\right) = X_3, \quad v_1\left(t_0^{(4)}\right) \geq 0, \quad v_1\left(t_f^{(4)}\right) = 0$$

$$x_2\left(t_0^{(4)}\right)=X_3,\quad x_2\left(t_f^{(4)}\right)=X_3,\quad v_2\left(t_0^{(4)}\right)=0,\quad v_2\left(t_f^{(4)}\right)=0$$

(c) the event constraints:

$$0\le v_n^{(p)}\le \bar{v},\quad n=1,2,\quad p=1,2,3,4$$

(d) the path constraints:

$$0\le F_1^{(p)}\le \hat{F}\left(v_1^{(p)}\right),\quad 0\le F_2^{(p)}\le \bar{F}\left(v_2^{(p)}\right),\quad p=1,2,3,4$$

$$0\le B_n^{(p)}\le \bar{B}\left(v_n^{(p)}\right),\quad n=1,2,\quad p=1,2,3,4$$

$$x_1^{(1)}-x_2^{(1)}\ge d,\quad x_2^{(3)}-x_1^{(3)}\ge d$$

and

(e) the linkage constraints:

$$t_f^{(p)}=t_0^{(p+1)},\quad p=1,2,3$$

$$x_n^{(p)}\left(t_f^{(p)}\right)=x_n^{(p+1)}\left(t_0^{(p+1)}\right),\quad v_n^{(p)}\left(t_f^{(p)}\right)=v_n^{(p+1)}\left(t_0^{(p+1)}\right),\quad n=1,2,\quad p=1,2,3$$

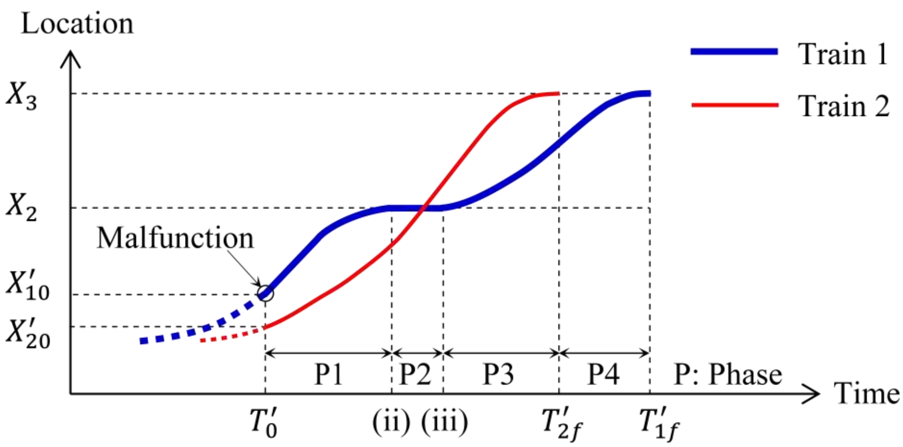

Figure 4. Illustration of phases under the modified schedule

The parameter values of GPOPS for solving the above MOCP are given in Table B.1 (column II). The computation time is 140 seconds. The result is shown in Figure 5. Train 1 stops at node 2 at 40km for about 1 minute (08:23-08:24), during which train 2 overtakes train 1 at a speed of about 150km/h. Both trains arrive at the destination as scheduled (08:45 for train 2 and 08:50 for train 1). The controls are also provided. It is clear that both trains applied coasting and maximum braking to stop at a node (nodes 2 and 3 for train 1, and node 3 for train 2). Specially, the control sequence for train 1 from node 2 to node 3 is maximum power - coasting - maximum braking, without using speedholding.

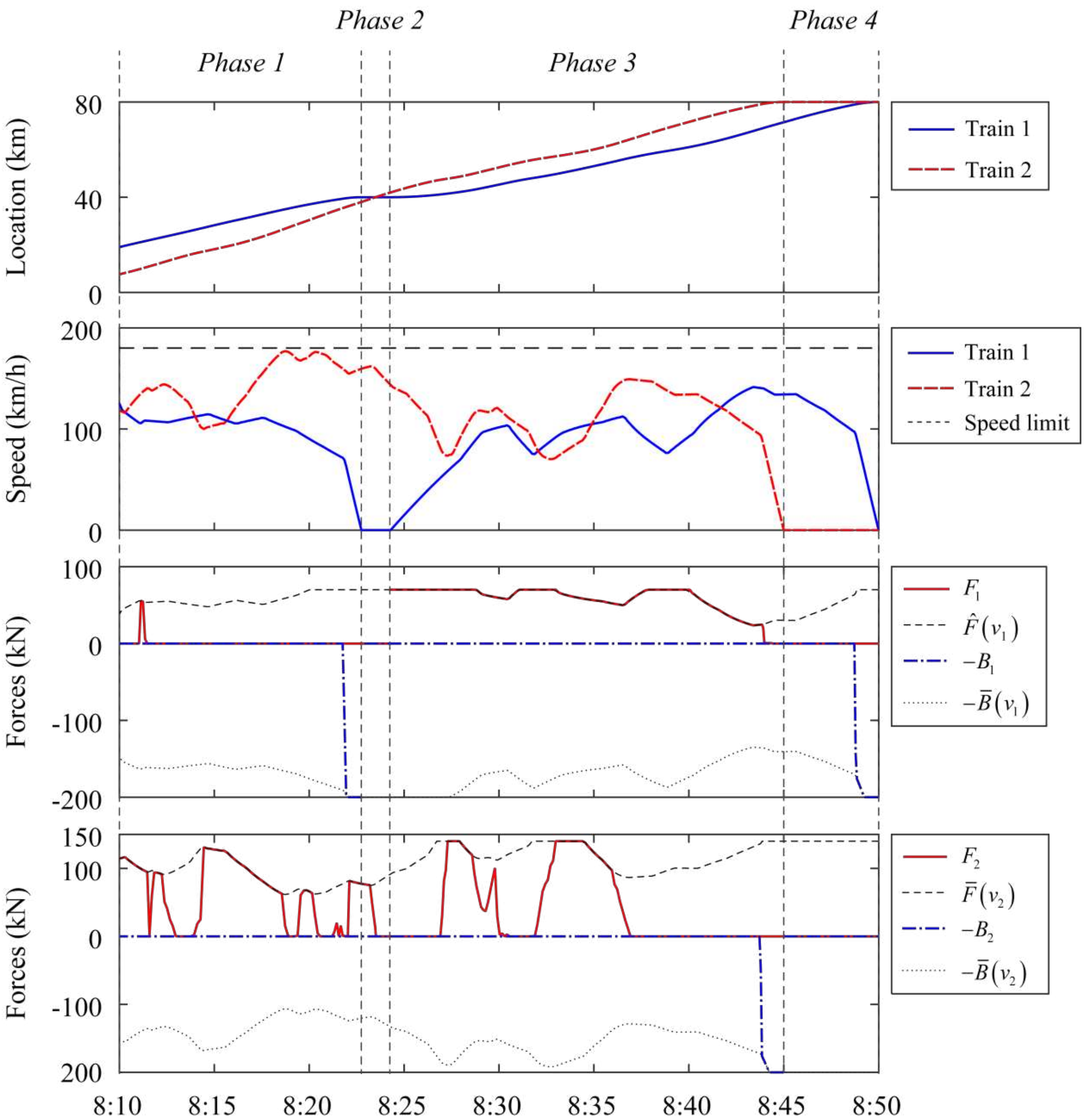

Figure 5. Optimal train trajectories and control under the rescheduled arrival times

4.2. Case study 2: integrated optimisation of schedules and control for single train

In this case study, we consider a combined scheduling and control problem for a single train traversing multiple stations. This situation can happen in the metro systems and high-speed railway systems, where the line is usually unidirectional, and trains running on each line are usually homogeneous and operated under an identical schedule. Under this circumstance, the trains would not interfere with each other, and we can consider the scheduling and control for only one train.

We choose the Yizhuang subway line in Beijing, China, as our study object. The entire line is 22728 meters long with 14 stations. For the parameter settings, we refer to previous literature on train scheduling and control with case studies conducted based on the Yizhuang line. The practical timetable is given in Table 6 (adopted from Li and Lo, 2014b), with a total running time of 2047 seconds. The data on track gradient and speed limit are adopted from Yang et al. (2015) and listed in Table 7 and Table 8, respectively. The train mass is $M = 2.78 \times 10^5$ kg (Wang et al. 2014). Functions of resistance (Wang et al., 2014), maximum tractive force (Su et al., 2015) and maximum braking force (Su et al., 2015) are given below, where v is in km/h, and $R(v)$, $\bar{F}(v)$ and $\bar{B}(v)$ are in kN.

$$R(v) = 2.2294 \times 10^{-3} v^2 + 3.9476$$

$$\bar{F}(v) = \begin{cases} 310, & 0 \le v \le 36 \\ 310 - 5(v - 36), & 36 < v \le 80 \end{cases}$$

$$\bar{B}(v) = \begin{cases} 260, & 0 \le v \le 60 \\ 260 - 5(v - 60), & 60 < v \le 80 \end{cases}$$

Table 6. Practical timetable of the Yizhuang line (adopted from Li and Lo, 2014b)

Station s	Station Name	Location X_s (m)	Arrival (s)	Departure (s)	Dwell (s)
1	Songjiazhuang (SJ)	0	-	0	-
2	Xiaocun (XC)	2631	190	220	30
3	Xiaohongmen (XH)	3905	328	358	30
4	Jiugong (JG)	6271	515	545	30
5	Yizhuangqiao (YZQ)	8254	680	715	35
6	Wenhuayuan (WH)	9246	805	835	30
7	Wanyuan (WY)	10785	949	979	30
8	Rongjing (RJ)	12065	1082	1112	30
9	Rongchang (RC)	13419	1216	1246	30
10	Tongjinan (TJ)	15756	1410	1440	30
11	Jinghai (JH)	18021	1590	1620	30
12	Ciqunan (CQN)	20107	1760	1795	35
13	Ciqu (CQ)	21394	1897	1942	45
14	Yizhuang (YZ)	22728	2047	-	-

Table 7. Speed limit in the form: speed (km/h)/subsection start – end location (m) (Yang et al., 2015)

50/0-150	85/150-480	65/480-1161	85/1161-2501	60/2501-2631	60/2631-2643
85/2643-2797	75/2797-3534	85/3534-3780	60/3780-3905	60/3905-3918	85/3918-5808
75/5808-6141	60/6141-6271	60/6271-6281	85/6281-8122	60/8122-8254	60/8254-8265
85/8265-9116	60/9116-9246	60/9246-9259	85/9259-10655	60/10655-10785	60/10785-10797
85/10797-11933	60/11933-12065	60/12065-12077	85/12077-13289	60/13289-13419	60/13419-13431
85/13431-14649	70/14649-15426	85/15426-15624	60/15624-15756	60/15756-15768	85/15768-17891
60/17891-18021	60/18021-18033	85/18033-19982	60/19982-20107	60/20107-20120	85/20120-21264
60/21264-21394	60/21394-21406	85/21406-22569	60/22569-22728		

Table 8. Track gradient in the form: gradient (‰)/subsection start – end location (m) (Yang et al., 2015)

-2/0-160	-3/160-470	10.4/470-970	3/970-1370	-8/1370-1880	3/1880-2500
-2/2500-2631	-2/2631-2770	-3/2770-3170	8.2/3170-3570	2/3570-3905	2/3905-3940
-20.4/3940-4200	-24/4200-4800	0/4800-5200	-2/5200-5800	-3.2/5800-6050	0/6050-6271
0/6271-6370	0/6271–6370	3.3/6370-6770	2.8/6770-7150	-15.6/7150-7415	9/7415-7675
0/7675-8254	0/8254-8376	5/8376-8736	-2/8736-9036	0/9036-9246	0/9246-9366
-2/9366-9806	5/9806-10126	3/10126-10606	0/10606-10785	0/10785-10866	2/10866-11426
-3/11426-11826	0/11826-12065	0/12065-12116	3.5/12116-12736	-1.8/12736-13116	0/13116-13419
0/13419-13526	-0.5/13526-13926	1.5/13926-14546	-1/14546-15176	6/15176-15476	0/15476-15756
0/15756-16006	-8/16006-16326	-3/16326-16696	5/16696-17136	1.4/17136-17816	0/17816-18021
0/18021-18136	15.5/18136-18486	24/18486-19186	-3/19186-19426	10.1/19426-19776	2/19776-20107
2/20107-20121	-3/20121-20796	3/20796-21231	2/21231-21394	2/21394-21481	20/21481-21681
3/21681-22066	-18.9/22066-22416	2/22416-22728			

With the original timetable, we are able to calculate the optimal train control and the minimum energy consumption. Since the running time on each section (which is the railway track between two consecutive metro stations) is fixed, the problem is solved as 13 single-phase optimal control problems with the parameter settings given in Table B.1 (column III). The computation time is 32 seconds. The minimum total energy consumption is 6.0977×10^8J. The optimal train speed profile and control strategy on each section are illustrated in Figure 6(a). The optimal control on most sections follows the sequence of maximum power - coasting - maximum braking. For some sections, the solutions become oscillatory, as illustrated in Figure 6(b). The oscillation on the JH-CQH section is corresponding to speedholding; while the oscillation on the CQ-YZ section may correspond to maximum traction.

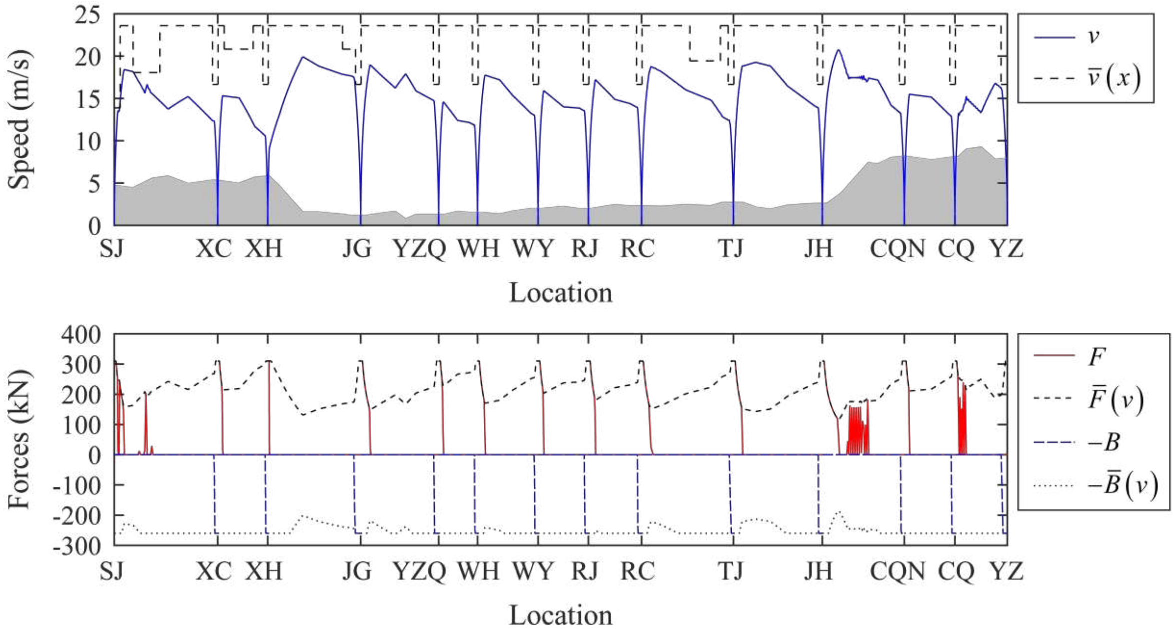

(a) The whole Yizhuang line

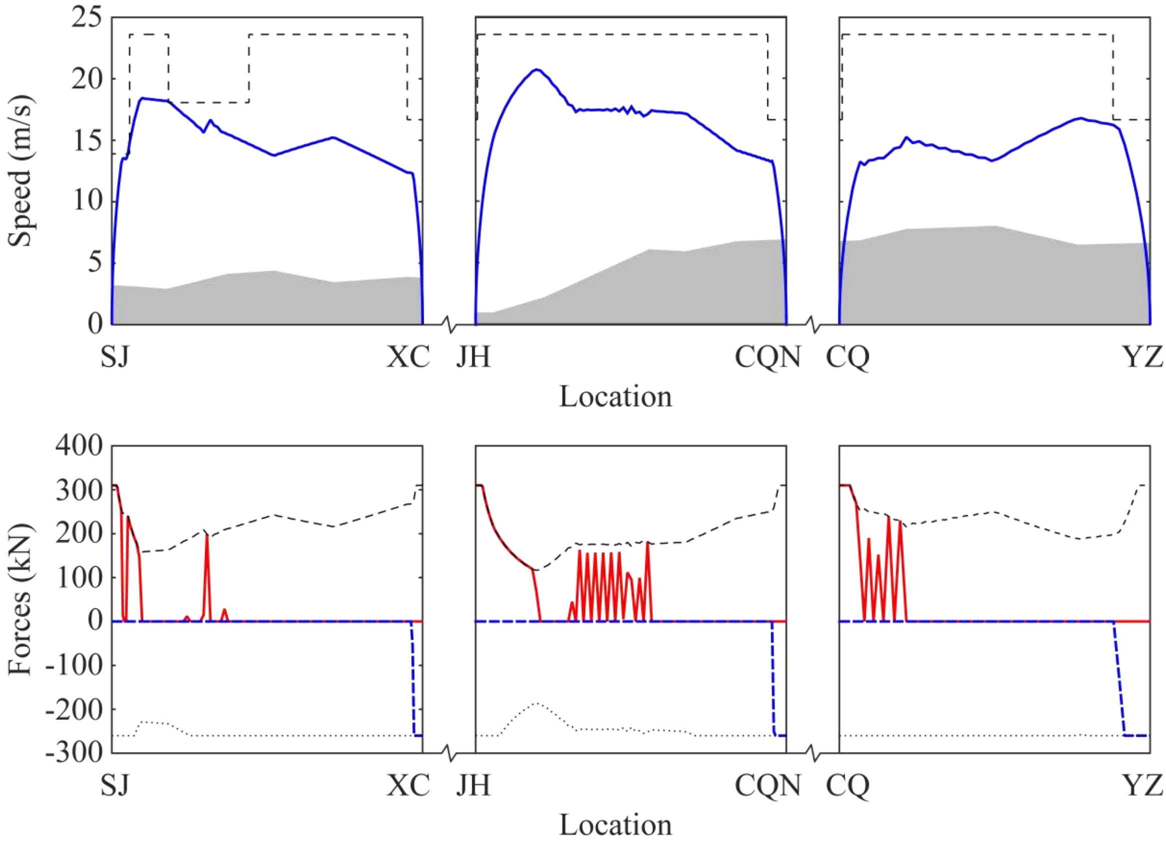

(b) Sections: SJ-XC, JH-CQN, CQ-YZ

Figure 6. Optimal speed and control with respect to location

We now see if we can further reduce the energy consumption by redistributing running times among different sections, while keeping the total running time and all the dwell times unchanged. A maximum adjustment of 30 seconds on running time is allowed on each section, while their sum should still be 1662 seconds (which is equal to the total running time minus the total dwell time). The maximum and minimum running times on each section i between stations i and $i+1$, denoted t_i^{max} and t_i^{min}, are listed in Table 9.

Table 9. Upper and lower bounds of running time on each section

Section i	1	2	3	4	5	6	7	8	9	10	11	12	13
t_i^{max} (s)	220	138	187	165	120	144	133	134	194	180	170	132	135
t_i^{min} (s)	160	78	127	105	60	84	73	74	134	120	110	72	75

To obtain the optimal running times and the corresponding control scheme, the MOCP with 13 phases is formulated as follows, where phase p corresponds to the journey on section p.

$$\min \sum_{p\in\mathbb{P}} \int_{t_0^{(p)}}^{t_f^{(p)}} F^{(p)}(t) v^{(p)}(t)\,dt\,, \quad \mathbb{P} = \{1, 2, \cdots, 13\} \tag{20}$$

subject to the dynamic constraints

$$\dot{x}^{(p)} = v^{(p)}, \quad p \in \mathbb{P} \tag{21}$$

$$\dot{v}^{(p)} = \frac{1}{M}\left[F^{(p)} - B^{(p)} - R\left(v^{(p)}\right) - G\left(x^{(p)}\right)\right], \quad p \in \mathbb{P} \tag{22}$$

the boundary constraints

$$t_0^{(1)} = 0\,, \quad t_f^{(13)} = 1662 \tag{23}$$

$$x\left(t_0^{(p)}\right) = X_p\,, \quad x\left(t_f^{(p)}\right) = X_{p+1}\,, \quad v\left(t_0^{(p)}\right) = v\left(t_f^{(p)}\right) = 0\,, \quad p \in \mathbb{P} \tag{24}$$

the event constraints

$$t_p^{min} \le t_f^{(p)} - t_0^{(p)} \le t_p^{max}\,, \quad p \in \mathbb{P} \tag{25}$$

$$v^{(p)} \ge 0\,, \quad F^{(p)} \ge 0\,, \quad B^{(p)} \ge 0\,, \quad p \in \mathbb{P} \tag{26}$$

the path constraints

$$v^{(p)} - \bar{v}\left(x^{(p)}\right) \le 0\,, \quad F^{(p)} - \bar{F}\left(v^{(p)}\right) \le 0\,, \quad B^{(p)} - \bar{B}\left(v^{(p)}\right) \le 0\,, \quad p \in \mathbb{P} \tag{27}$$

and the linkage constraints

$$t_f^{(p)} = t_0^{(p+1)}\,, \quad p \in \mathbb{P} \setminus \{13\} \tag{28}$$

Problem (20)-(28) is solved by GPOPS with the parameter settings given in Table B.1 (column IV), and the computation time is 174 seconds. The optimal running time in each section is given in Table 10, where the offset is defined as the optimal running time minus the original running time on each section. With this optimised timetable, the train control is recalculated as the single-phase problems with parameters given in Table B.1 (column III), and the computation time is 32 seconds. The minimum energy consumption under the optimal timetable is 6.0811×10^8J, which is equal to a reduction of 0.27% compared to that under the original timetable in Table 6. Interpretation of this result can be twofold: either the original timetable is already quite energy efficient, or the optimised timetable is only a sub-optimal solution. To uncover the exact reason requires further development on the solution algorithms in the future.

Table 10. Optimal running times and the offsets to the original ones

Section	1	2	3	4	5	6	7	8	9	10	11	12	13
Optimal (s)	173	105	147	138	91	118	106	109	157	152	148	105	113
Offset (s)	-17	-3	-10	3	1	4	3	5	-7	2	8	3	8

5. Conclusions

In this paper, we formulated the multi-train scheduling and control problem as a MOCP to achieve minimum energy consumption in a moving-block system with multiple nodes, by assuming a predetermined departure/arrival sequence of all trains at all nodes. The practical track conditions, train dynamics and operation constraints are considered. Two case studies are conducted to demonstrate the feasibility of this framework in solving practical problems.

As it was revealed in the case studies, the optimal control obtained from the pseudospectral method may behave unexpected fluctuation. For future research, we are interested in designing algorithms tailored for the proposed MOCP to provide better solutions. For example, pre-analysis on the optimal strategy, such as what have been done in Albrecht et al. (2015b, 2015c), Gu et al. (2014), Howlett et al. (2009), Khmelnitsky (2000), and Liu and

Golovitcher (2003), can be used in conjunction with mathematical programming methods. On the other hand, although the proposed MOCP framework is suitable for modelling very complex train networks, the case studies we provided were still based on simple scenarios with a small number of trains and/or nodes. Increasing the number of trains and/or nodes would significantly increase the number of phases, which further requires algorithms of greater efficiency and pre-analysis on the MOCP itself. A possible strategy may be to divide the original MOCP into sub-MOCPs by analysing the relations of the trains over different phases.

Further, the requirement of a prescribed D/A-sequence for the proposed framework means that it cannot be directly deployed for the energy-based scheduling in a complex railway network. Instead, it can be embedded in a bi-level scheduling process, where the upper level generates the D/A-sequence, and the lower level uses the method proposed in this paper to evaluate the energy efficiency of the generated D/A-sequence.

It is also worth pointing out that, the modelling technique established in this paper can be useful to not only the railway operation but a wider transportation area. For example, He et al. (2015) used multiphase optimal control to optimise the individual vehicular trajectories along a signalised urban road corridor, and the MOCP they established is similar to that we have formulated in the second case study.

Acknowledgements

The authors wish to express their thanks to the two anonymous reviewers for their useful comments on the earlier versions of this paper. The work described in this paper was supported by the UK Rail Safety and Standards Board, Grant No. T1071.

Appendix A. Introduction to the Radau pseudospectral method

The Radau pseudospectral method (RPM) is a pseudospectral method (Rao, 2009) whose collocation points are the Legendre-Gauss-Radau (LGR) points. We refer to Garg et al. (2010, 2011a, 2011b) and Patterson and Rao (2012, 2014) for the main idea of RPM. For the sake of presentation, we restate the MOCP as follows with a new, and more general, set of notations.

Consider a MOCP of P phases, and denote by $t_0^{(p)}$, $t_f^{(p)}$, $x^{(p)}$ and $u^{(p)}$ the start time, end time, state and control of phase $p=1,2,\cdots,P$. The objective is

$$\min J = \sum_{p=1}^{P}\left[\Phi^{(p)}\left(x^{(p)}\left(t_0^{(p)}\right),t_0^{(p)},x^{(p)}\left(t_f^{(p)}\right),t_f^{(p)}\right)+\int_{t_0^{(p)}}^{t_f^{(p)}}\varphi^{(p)}\left(x^{(p)}(t),u^{(p)}(t),t\right)dt\right] \quad (A.1)$$

subject to the dynamic constraints

$$\dot{x}^{(p)} = f^{(p)}\left(x^{(p)}(t),u^{(p)}(t),t\right),\quad p=1,\cdots,P \quad (A.2)$$

the inequality path constraints

$$C_{\min}^{(p)} \le C^{(p)}\left(x^{(p)}(t),u^{(p)}(t),t\right) \le C_{\max}^{(p)},\quad p=1,\cdots,P \quad (A.3)$$

the boundary constraints

$$\phi_{\min}^{(p)} \le \phi^{(p)}\left(x^{(p)}\left(t_0^{(p)}\right),t_0^{(p)},x^{(p)}\left(t_f^{(p)}\right),t_f^{(p)}\right) \le \phi_{\max}^{(p)},\quad p=1,\cdots,P \quad (A.4)$$

and the linkage constraints[11]

$$t_f^{(p)} = t_0^{(p+1)},\quad x^{(p)}\left(t_f^{(p)}\right) = x^{(p+1)}\left(t_0^{(p+1)}\right),\quad p=1,\cdots,P-1 \quad (A.5)$$

Let $\tau=[-1,1]$ be a new independent variable. Variable t can then be defined in terms of τ as

$$t = \frac{t_f^{(p)}-t_0^{(p)}}{2}\tau + \frac{t_f^{(p)}+t_0^{(p)}}{2}$$

and the MOCP (A.1)-(A.5) is defined in terms of τ as

$$\min J = \sum_{p=1}^{P}\left[\Phi^{(p)}\left(x^{(p)}(-1),t_0^{(p)},x^{(p)}(1),t_f^{(p)}\right)+\frac{t_f^{(p)}-t_0^{(p)}}{2}\int_{-1}^{1}\varphi^{(p)}\left(x^{(p)}(\tau),u^{(p)}(\tau),\tau;t_0^{(p)},t_f^{(p)}\right)d\tau\right] \quad (A.6)$$

subject to the dynamic constraints

$$\dot{x}^{(p)} = \frac{t_f^{(p)}-t_0^{(p)}}{2} f^{(p)}\left(x^{(p)}(\tau),u^{(p)}(\tau),\tau;t_0^{(p)},t_f^{(p)}\right),\quad p=1,\cdots,P \quad (A.7)$$

the inequality path constraints

$$C_{\min}^{(p)} \le C^{(p)}\left(x^{(p)}(\tau),u^{(p)}(\tau),\tau;t_0^{(p)},t_f^{(p)}\right) \le C_{\max}^{(p)},\quad p=1,\cdots,P \quad (A.8)$$

the boundary constraints

[11] For a more general form of the linkage constraints, please see Betts (2010) and Rao et al. (2010).

$$\phi_{min}^{(p)} \le \phi^{(p)}\left(x^{(p)}(-1), t_0^{(p)}, x^{(p)}(1), t_f^{(p)}\right) \le \phi_{max}^{(p)}, \quad p = 1, \cdots, P \tag{A.9}$$

and the linkage constraints

$$t_f^{(p)} = t_0^{(p+1)}, \quad x^{(p)}(1) = x^{(p+1)}(-1), \quad p = 1, \cdots, P-1 \tag{A.10}$$

Problem (A.6)-(A.10) will then be discretised by RPM and solved as a nonlinear programming problem. The remainder of this appendix will focus on the discretisation of a specific phase p, and the superscript p as the phase identifier will be omitted unless it is needed to distinguish among phases.

Denote $N^{(p)}$ as the number of LGR collocation points for phase p. Then the LGR points, denoted $-1 = \tau_1 < \cdots < \tau_N < 1$, would be the roots of $Q_{N-1}(\tau) + Q_N(\tau)$ where

$$Q_N(\tau) = \frac{1}{2^N N!} \frac{d^N}{d\tau^N}\left[\left(\tau^2 - 1\right)^N\right] \tag{A.11}$$

The LGR collocation points, together with the noncollocated point $\tau_{N+1} = 1$, are used for RPM. Associated with each LGR point τ_i is the LGR weight ω_i computed as (Garg, 2011)

$$\omega_i = \begin{cases} \dfrac{2}{N^2} & i = 1 \\ \dfrac{1}{(1-\tau_i)\left[Q'_{N-1}(\tau_i)\right]^2} & 2 \le i \le N \end{cases} \tag{A.12}$$

Denote by X_i and U_i the approximation of state and control at τ_i, respectively, then $x(\tau)$ is approximated by

$$x(\tau) \approx \sum_{i=1}^{N+1} X_i L_i(\tau) \tag{A.13}$$

where $L_i(\tau)$, $i = 1, \cdots, N+1$, is defined as

$$L_i(\tau) = \prod_{j=1, j\ne i}^{N+1} \frac{\tau - \tau_j}{\tau_i - \tau_j}, \quad i = 1, \cdots, N+1 \tag{A.14}$$

By substituting Eqs. (A.13) and (A.14) into Eq. (A.7), the dynamic constraints are approximated at the LGR points as

$$\dot{x}(\tau_k) \approx \sum_{i=1}^{N+1} X_i \dot{L}_i(\tau_k) = \frac{t_f - t_0}{2} f\left(X_k, U_k, \tau_k; t_0^{(p)}, t_f^{(p)}\right), \quad k = 1, \cdots, N \tag{A.15}$$

where $\dot{L}_i(\tau_k)$ is the derivative of $L_i(\tau)$ evaluated at $\tau = \tau_k$. The cost function in Eq. (A.6) is approximated by

$$J = \sum_{p=1}^{P} \left[\Phi^{(p)}\left(X_1^{(p)}, t_0^{(p)}, X_{N^{(p)}+1}^{(p)}, t_f^{(p)}\right) + \frac{t_f^{(p)} - t_0^{(p)}}{2} \sum_{k=1}^{N^{(p)}} \omega_k \varphi^{(p)}\left(X_k^{(p)}, U_k^{(p)}, \tau_k; t_0^{(p)}, t_f^{(p)}\right) \right] \tag{A.16}$$

Furthermore, the path constraints in Eq. (A.3) are approximated at the LGR points as

$$C_{\min}^{(p)} \le C^{(p)}\left(X_k^{(p)}, U_k^{(p)}, \tau_k^{(p)}; t_0^{(p)}, t_f^{(p)}\right) \le C_{\max}^{(p)}, \quad k = 1, \cdots, N^{(p)}, \quad p = 1, \cdots, P \tag{A.17}$$

the boundary constraints in Eq. (A.4) are approximated as

$$\phi_{\min}^{(p)} \le \phi\left(X_1^{(p)}, t_0^{(p)}, X_{N^{(p)}+1}^{(p)}, t_f^{(p)}\right) \le \phi_{\max}^{(p)}, \quad p = 1, \cdots, P \tag{A.18}$$

and the linkage constraints in Eq. (A.5) now read

$$t_f^{(p)} = t_0^{(p+1)}, \quad X_{N^{(p)}+1}^{(p)} = X_1^{(p+1)}, \quad p = 1, \cdots, P-1 \tag{A.19}$$

By now, the MOCP (A.6)-(A.10) is converted to the following nonlinear programming (NLP) problem,

$$\min \text{ Eq. (A.16) s.t. Eqs. (A.11)-(A.12), (A.14)-(A.19)} \tag{A.20}$$

and the decision variables are $t_0^{(p)}$, $t_f^{(p)}$, $X_1^{(p)}, \cdots, X_{N^{(p)}+1}^{(p)}$, $U_1^{(p)}, \cdots, U_{N^{(p)}}^{(p)}$, $p = 1, \cdots, P$. Techniques of solving this NLP problem is not further introduced in this paper but can be found in Patterson and Rao (2012, 2014) and references therein.

Appendix B. Parameter settings for the case studies

Referring to Table B.1, the key parameters of GPOPS Version 5.1 are explained as follows:

(i) setup.autoscale indicates whether the MOCP is scaled automatically before it is solved. limits(p).nodesPerInterval specifies the number of collocation points in each phase p.

(ii) limits(p).meshPoints and setup.mesh.iteration are paramerters for the hp-adaptive mesh refinement (Darby et al., 2011; Patterson et al., 2015). The former specifies the mesh points of each phase p for the initial run of GPOPS, and the latter gives the number of iterations for performing the mesh refinement. Considering the computational effort as well as the operability of the solutions, the hp-adaptive mesh refinement is excluded in the case studies by appropriate parameter settings.

(iii) setup.derivatives and setup.tolerances are parameters for solving the NLP problem. The former indicates the approach to computing the derivatives of the objective function and the constraints of the NLP problem. The latter is a row vector of two elements which respectively specify the optimality and feasibility tolerances of the NLP solver: for SNOPT used by GPOPS Version 5.1, they should be the Major optimality tolerance and the Major feasibility tolerance (Gill et al., 2005).

When solving the case study problems, the performance of GPOPS, in terms of computation time as well as the accuracy and operability of the solution, is sensitive to the parameters of GPOPS and the settings of the problem itself. As a result, choosing the appropriate parameters for GPOPS is a tedious trial-and-error process. We choose the optimality and feasibility tolerances as small as possible while assuring that they can be satisfied when the NLP solver terminated. As we can see, for columns I/II/IV, the feasibility tolerance is reasonably small to assure a feasible solution; while the not-so-small optimality tolerance may indicate a sub-optimal solution.

Table B.1. Parameter settings for GPOPS Version 5.1 in the case studies

Parameter	I	II	III	IV
setup.autoscale	'off'	'off'	'off'	'off'
limits(p).nodesPerInterval	440 (p=1)	110 (p=1,2) 230 (p=3) 100 (p=4)	60/80/100/140/150/190* (p=1)	100 (p=1,2,···,13)
setup.mesh.iteration	0	0	0	0
limits(p).meshPoints	[-1,1] (p=1)	[-1,1] (p=1,2,3,4)	[-1,1] (p=1)	[-1,1] (p=1,2,···,13)
setup.derivatives	'complex'	'complex'	'complex'	'complex'
setup.tolerances	[4.2e-3, 2.5e-4]	[6.3e-3, 1.2e-4]	[2e-6, 5e-12]	[4.7e-4, 3.1e-5]

* 60 for section 9; 80 for section 13; 100 for section 5; 140 for sections 2/3/6/7/8/11/12; 150 for section 1; 190 for sections 4/10.

References

Açıkbaş, S., Söylemez, M.T., 2008. Coasting point optimisation for mass rail transit lines using artificial neural networks and genetic algorithms. IET Electric Power Applications 2 (3), 172-182.

Albrecht, A., Howlett, P., Pudney, P., 2016. The cost-time curve for an optimal train journey on level track. The ANZIAM Journal (in press)

Albrecht, A.R., Howlett, P.G., Pudney, P.J., Vu, X., Zhou, P., 2015a. Energy-efficient train control: The two-train separation problem on level track. Journal of Rail Transport Planning & Management 5 (3), 163-182.

Albrecht, A., Howlett, P., Pudney, P., Vu, X., Zhou, P., 2015b. The key principles of optimal train control-Part 1: Formulation of the model, strategies of optimal type, evolutionary lines, location of optimal switching points. Transportation Research Part B (in press)

Albrecht, A., Howlett, P., Pudney, P., Vu, X., Zhou, P., 2015c. The key principles of optimal train control-Part 2: Existence of an optimal strategy, the local energy minimization principle, uniqueness, computational techniques. Transportation Research Part B (in press)

Asnis, I.A., Dmitruk, A.V., Osmolovskii, N.P., 1985. Solution of the problem of the energetically optimal control of the motion of a train by the maximum principle. USSR Computational Mathematics and Mathematical Physics 25 (6), 37-44.

Becerra, V.M., 2010. Solving complex optimal control problems at no cost with PSOPT. 2010 IEEE International Symposium on Computer-Aided Control System Design, pp. 1391-1396.

Benson, D.A., Huntington, G.T., Thorvaldsen, T.P., Rao, A.V., 2006. Direct trajectory optimization and costate estimation via an orthogonal collocation method. Journal of Guidance, Control, and Dynamics 29 (6), 1435-1440.

Betts, J., 2010. Practical Methods for Optimal Control and Estimation using Nonlinear Programming. Society for Industrial and Applied Mathematics.

Cacchiani, V., Huisman, D., Kidd, M., Kroon, L., Toth, P., Veelenturf, L., Wagenaar, J., 2014. An overview of recovery models and algorithms for real-time railway rescheduling. Transportation Research Part B 63, 15-37.

Cacchiani, V., Toth, P., 2012. Nominal and robust train timetabling problems. European Journal of Operational Research 219 (3), 727-737.

Carey, M., 1994. A model and strategy for train pathing with choice of lines, platforms, and routes. Transportation Research Part B 28 (5), 333-353.

Chang, C.S., Sim, S.S., 1997. Optimising train movements through coast control using genetic algorithms. IEE Proceedings - Electric Power Applications, 144 (1), 65-73.

Chen, J., Liu, R., Ngoduy, D., Shi, Z., 2016. A new multi-anticipative car-following model with consideration of the desired following distance. Nonlinear Dynamics (in press)

Cheng, J., Davydova, Y., Howlett, P., Pudney, P., 1999. Optimal driving strategies for a train journey with non-zero track gradient and speed limits. IMA Journal of Management Mathematics 10 (2), 89-115.

Cheng, J., Howlett, P., 1992. Application of critical velocities to the minimisation of fuel consumption in the control of trains. Automatica 28 (1), 165-169.

Cheng, J., Howlett, P., 1993. A note on the calculation of optimal strategies for the minimization of fuel consumption in the control of trains. IEEE Transactions on Automatic Control 38 (11), 1730-1734.

Darby, C.L., Hager, W.W., Rao, A.V., 2011. An hp-adaptive pseudospectral method for solving optimal control problems. Optimal Control Applications and Methods 32 (4), 476-502.

Dorfman, M.J., Medanic, J., 2004. Scheduling trains on a railway network using a discrete event model of railway traffic. Transportation Research Part B 38 (1), 81-98.

Effati, S., Roohparvar, H., 2006. The minimization of the fuel costs in the train transportation. Applied Mathematics and Computation 175 (2), 1415-1431.

Franke, R., Terwiesch, P., Meyer, M., 2000. An algorithm for the optimal control of the driving of trains. Proceedings of the 39th IEEE Conference on Decision and Control, 2000, vol.3, pp. 2123-2128.

Garg, D., 2011. Advances in Global Pseudospectral Methods for Optimal Control. PhD Thesis. University of Florida.

Garg, D., Hager, W.W., Rao, A.V., 2011a. Pseudospectral methods for solving infinite-horizon optimal control problems. Automatica 47 (4), 829-837.

Garg, D., Patterson, M., Francolin, C., Darby, C., Huntington, G., Hager, W., Rao, A., 2011b. Direct trajectory optimization and costate estimation of finite-horizon and infinite-horizon optimal control problems using a Radau pseudospectral method. Computational Optimization and Applications 49 (2), 335-358.

Garg, D., Patterson, M., Hager, W.W., Rao, A.V., Benson, D.A., Huntington, G.T., 2010. A unified framework for the numerical solution of optimal control problems using pseudospectral methods. Automatica 46 (11), 1843-1851.

Ghoseiri, K., Szidarovszky, F., Asgharpour, M.J., 2004. A multi-objective train scheduling model and solution. Transportation Research Part B 38 (10), 927-952.

Gill, P., Murray, W., Saunders, M., 2005. SNOPT: An SQP algorithm for large-scale constrained optimization. SIAM Review 47 (1), 99-131.

Goodwin, J.C.J., Fletcher, D.I., Harrison, R.F., 2016. Multi-train trajectory optimisation to maximise rail network energy efficiency under travel-time constraints. Journal of Rail and Rapid Transit 230 (4), 1318-1335.

Gu, Q., Tang, T., Cao, F., Song, Y.D., 2014. Energy-efficient train operation in urban rail transit using real-time traffic information. IEEE Transactions on Intelligent Transportation Systems 15 (3), 1216-1233.

Guo, X., Wu, J., Sun, H., Liu, R., Gao, Z., 2016. Timetable coordination of first trains in urban railway network: A case study of Beijing. Applied Mathematical Modelling (in press)

Gupta, S.D., Tobin, J.K., Pavel, L., 2016. A two-step linear programming model for energy-efficient timetables in metro railway networks. Transportation Research Part B 93, 57-74.

He, X., Liu, H.X., Liu, X., 2015. Optimal vehicle speed trajectory on a signalized arterial with consideration of queue. Transportation Research Part C 61, 106-120.

Higgins, A., Kozan, E., Ferreira, L., 1996. Optimal scheduling of trains on a single line track. Transportation Research Part B 30 (2), 147-161.

Howlett, P., 1990. An optimal strategy for the control of a train. The ANZIAM Journal 31 (04), 454-471.

Howlett, P., 1996. Optimal strategies for the control of a train. Automatica 32 (4), 519-532.

Howlett, P., 2000. The optimal control of a train. Annals of Operations Research 98 (1-4), 65-87.

Howlett, P.G., Cheng, J., 1997. Optimal driving strategies for a train on a track with continuously varying gradient. The ANZIAM Journal 38 (03), 388-410.

Howlett, P.G., Pudney, P.J., 1995. Energy-Efficient Train Control. Springer, New York.

Howlett, P.G., Pudney, P.J., Vu, X., 2009. Local energy minimization in optimal train control. Automatica 45 (11), 2692-2698.

Ichikawa, K., 1968. Application of optimization theory for bounded state variable problems to the operation of train. Bulletin of JSME 11 (47), 857-865.

Jaekel, B., Albrecht, T., 2014. Comparative analysis of algorithms and models for train running simulation. Journal of Rail Transport Planning & Management 4 (1-2), 14-27.

Khmelnitsky, E., 2000. On an optimal control problem of train operation. IEEE Transactions on Automatic Control 45 (7), 1257-1266.

Ko, H., Koseki, T., Miyatake, M., 2004. Application of dynamic programming to the optimization of the running profile of a train. Computers in Railways IX, WIT Press, 103-112.

Li, F., Gao, Z., Li, K., Yang, L., 2008. Efficient scheduling of railway traffic based on global information of train. Transportation Research Part B 42 (10), 1008-1030.

Li, X., Lo, H.K., 2014a. An energy-efficient scheduling and speed control approach for metro rail operations. Transportation Research Part B 64, 73-89.

Li, X., Lo, H.K., 2014b. Energy minimization in dynamic train scheduling and control for metro rail operations. Transportation Research Part B 70, 269-284.

Liu, R., Golovitcher, I.M., 2003. Energy-efficient operation of rail vehicles. Transportation Research Part A 37 (10), 917-932.

Lu, Q., Feng, X., 2011. Optimal control strategy for energy saving in trains under the four-aspect fixed autoblock system. Journal of Modern Transportation 19 (2), 82-87.

Medanic and Dorfman, 2002. Efficient scheduling of traffic on a railway line. Journal of Optimization Theory and Applications 115 (3), 587-602.

Milroy, I.P., 1980. Aspects of Automatic Train Control. PhD Thesis, Loughborough University.

Miyatake, M., Ko, H., 2010. Optimization of train speed profile for minimum energy consumption. IEEJ Transactions on Electrical and Electronic Engineering 5 (3), 263-269.

Patterson, M.A., Hager, W.W., Rao, A.V., 2015. A ph mesh refinement method for optimal control. Optimal Control Applications and Methods 36 (4), 398-421.

Patterson, M.A., Rao, A.V., 2012. Exploiting sparsity in direct collocation pseudospectral methods for solving optimal control problems. Journal of Spacecraft and Rockets 49 (2), 354-377.

Patterson, M.A., Rao, A.V., 2014. GPOPS-II: A Matlab software for solving multiple-phase optimal control problems using hp-adaptive Gaussian quadrature collocation methods and sparse nonlinear programming. ACM Transactions on Mathematical Software 41 (1), 1-37.

Pudney, P., Howlett, P., 1994. Optimal driving strategies for a train journey with speed limits. The ANZIAM Journal 36 (01), 38-49.

Rao, A.V., Benson, D.A., Darby, C., Patterson, M.A., Francolin, C., Sanders, I., Huntington, G.T., 2010. Algorithm 902: GPOPS, A MATLAB software for solving multiple-phase optimal control problems using the Gauss pseudospectral method. ACM Transactions on Mathematical Software. 37 (2), 22:1-22:39.

Rao, A.V., 2009. A survey of numerical methods for optimal control. Advances in the Astronautical Sciences 135 (1), 497-528.

Rochard, B.P., Schmid, F., 2000. A review of methods to measure and calculate train resistances. Journal of Rail and Rapid Transit 214 (4), 185-199.

Su, S., Li, X., Tang, T., Gao, Z., 2013. A subway train timetable optimization approach based on energy-efficient operation strategy. IEEE Transactions on Intelligent Transportation Systems 14 (2), 883-893.

Su, S., Tang, T., Roberts, C., 2015. A cooperative train control model for energy saving. IEEE Transactions on Intelligent Transportation Systems 16 (2), 622-631.

Vasak, M., Baotic, M., Peric, N., Bago, M., 2009. Optimal rail route energy management under constraints and fixed arrival time. 2009 European Control Conference (ECC), pp. 2972-2977.

Wang, P., Goverde, R.M.P., 2016. Multiple-phase train trajectory optimization with signalling and operational constraints. Transportation Research Part C 69, 255-275.

Wang, Y., De Schutter, B., van den Boom, T.J.J., Ning, B., 2013. Optimal trajectory planning for trains - A pseudospectral method and a mixed integer linear programming approach. Transportation Research Part C 29, 97-114.

Wang, Y., De Schutter, B., van den Boom, T.J.J., Ning, B., 2014. Optimal trajectory planning for trains under fixed and moving signaling systems using mixed integer linear programming. Control Engineering Practice 22, 44-56.

Wong, K.K., Ho, T.K., 2004. Dynamic coast control of train movement with genetic algorithm. International Journal of Systems Science 35 (13-14), 835-846.

Xu, X., Li, K., Li, X., 2016. A multi-objective subway timetable optimization approach with minimum passenger time and energy consumption. Journal of Advanced Transportation 50 (1), 69-95.

Yan, X., Cai, B., Ning, B., ShangGuan, W., 2016. Online distributed cooperative model predictive control of energy-saving trajectory planning for multiple high-speed train movements. Transportation Research Part C 69, 60-78.

Yang, L., Li, K., Gao, Z., Li, X., 2012. Optimizing trains movement on a railway network. Omega 40 (5), 619-633.

Yang, X., Chen, A., Ning, B., Tang, T., 2016. A stochastic model for the integrated optimization on metro timetable and speed profile with uncertain train mass. Transportation Research Part B 91, 424-445.

Yang, X., Li, X., Ning, B., Tang, T., 2015. An optimisation method for train scheduling with minimum energy consumption and travel time in metro rail systems. Transportmetrica B 3 (2), 79-98.

Yin, J., Tang, T., Yang, L., Gao, Z., Ran, B., 2016. Energy-efficient metro train rescheduling with uncertain time-variant passenger demands: An approximate dynamic programming approach. Transportation Research Part B 91, 178-210.

Zhao, N., Roberts, C., Hillmansen, S., Nicholson, G., 2015. A multiple train trajectory optimization to minimize energy consumption and delay. IEEE Transactions on Intelligent Transportation Systems, 16 (5), 2363-2372.